

Search for NN -decoupled dibaryons using the process $pp \rightarrow \gamma\gamma X$ below the pion production threshold

A.S.Khrykin, V.F.Boreiko, Yu.G.Budyashov, S.B.Gerasimov,
N.V.Khomutov, Yu.G.Sobolev, V.P.Zorin

November 20, 2018

Abstract

The energy spectrum for high energy γ -rays ($E_\gamma \geq 10$ MeV) from the process $pp \rightarrow \gamma\gamma X$ emitted at 90° in the laboratory frame has been measured at an energy below the pion production threshold, namely, at 216 MeV. The resulting photon energy spectrum extracted from $\gamma-\gamma$ coincidence events consists of a narrow peak at a photon energy of about 24 MeV and a relatively broad peak in the energy range of (50 - 70) MeV. The statistical significances for the narrow and broad peaks are 5.3σ and 3.5σ , respectively. This behavior of the photon energy spectrum is interpreted as a signature of the exotic dibaryon resonance d_1^* with a mass of about 1956 MeV which is assumed to be formed in the radiative process $pp \rightarrow \gamma d_1^*$ followed by its electromagnetic decay via the $d_1^* \rightarrow pp\gamma$ mode. The experimental spectrum is compared with those obtained by means of Monte Carlo simulations.

1 Introduction

Direct-production of two hard photons in nucleon-nucleon collisions ($NN\gamma\gamma$) at intermediate energies, unlike production of single photons (NN bremsstrahlung), is one of those fundamental processes which are still poorly explored both theoretically and experimentally. However, a study of this process can yield new important information on the underlying mechanisms of the NN interaction that is complementary to that obtained from investigations of other processes. In particular, the $NN\gamma\gamma$ process can be used as a sensitive probe for experimental verification of the possible existence of NN -decoupled nonstrange dibaryon resonances. These are two-baryon states 2B

with zero strangeness and exotic quantum numbers, for which the strong decay ${}^2B \rightarrow NN$ is either strictly forbidden by the Pauli principle (for the states with the isospin $I = 1(0)$ and with an even sum $L + S + I$, where L is the orbital momentum and S is the spin), or is strongly suppressed by the isospin selection rules (for the states with $I = 2$)[1, 2]. Such dibaryon states cannot be simple bound systems of two color-singlet nucleons, and a proof of their existence would have consequences of fundamental significance for the theory of strong interactions. The NN -decoupled dibaryon states are predicted in a series of QCD -inspired models[3, 4, 5]. Among the predicted dibaryons, there are those with masses both below and above the pion production (πNN) threshold. The NN -decoupled dibaryons with masses below the πNN threshold are of special interest, since they may decay mainly into the $NN\gamma$ state, and consequently, their widths should be very narrow ($\leq 1keV$). Narrow dibaryon states have been searched for in a number of experiments[6], but none has provided any convincing evidence for their existence. Most of the past searches, however, were limited to dibaryons coupled to the NN channel, and, to our knowledge, only a few were dedicated to the NN -decoupled dibaryons[7, 8, 9]. At the same time, since the dibaryons we are interested in do not couple to the NN -channel, then, depending on their production and decay modes, they may have escaped detection up to now and may naturally appear in dedicated experiments.

If the NN -decoupled dibaryons exist in nature, then the $NN\gamma\gamma$ process may proceed, at least partly, through the mechanism that directly involves the radiative excitation $NN \rightarrow \gamma {}^2B$ and decay ${}^2B \rightarrow \gamma NN$ modes of these states. In NN collisions at energies below the πNN threshold, these production and decay modes of the NN -decoupled dibaryon resonances with masses $M_R \leq 2m_N + m_\pi$ would be unique or dominant. The simplest and clear way of revealing them is to measure the photon energy spectrum of the reaction $NN\gamma\gamma$. The presence of an NN -decoupled dibaryon resonance would reveal itself in this energy spectrum as a narrow line associated with the formation of this resonance and a relatively broad peak originating from its three-particle decay. In the center-of-mass system, the position of the narrow line(E_R) is determined by the energy of colliding nucleons ($W = \sqrt{s}$) and the mass of this dibaryon resonance as $E_R = (W^2 - M_R^2)/2W$. An essential feature of the two-photon production in NN collisions at an energy below the pion production threshold is that, apart from the resonant mechanism in question, there should only be one more source of photon pairs. This is the double NN -bremsstrahlung reaction. But this reaction is expected to play a minor role. Indeed, it involves two electromagnetic vertices, so that one may expect that the $NN\gamma\gamma$ -to- $NN\gamma$ cross section ratio should be of the order of the fine structure constant α . However, the cross section for $NN\gamma$ is already

small (for example, the total pp -bremsstrahlung cross section at energies of interest is a few μb).

The process $pp \rightarrow pp\gamma\gamma$ at an energy below the pion production threshold provides an unique possibility of searching for the NN -decoupled dibaryon resonances in the mass region $M_R \leq 2m_p + m_\pi$ with quantum numbers $I(J^P) = 1(1^+, 3^+, \text{etc.})$ or those with $I = 2$ (J is the total spin, and P is the parity of a dibaryon). The preliminary experimental studies of the reaction $pp \rightarrow \gamma\gamma X$ at an incident proton energy of about 200 MeV[10, 11] showed that the photon energy spectrum of this reaction had a peculiar structure ranging from about 20 MeV to about 60 MeV. This structure was interpreted as an indication of the possible existence of an NN -decoupled dibaryon resonance (later called d_1^*) that is produced in the process $pp \rightarrow \gamma d_1^*$ and subsequently decays via the $d_1^* \rightarrow pp\gamma$ channel. Unfortunately, a relatively coarse energy resolution and low statistics did not allow us to distinguish the narrow γ -peak associated with the d_1^* production from the broad γ -peak due to the decay of this resonance and, hence, to determine the resonance mass exactly. To get a rough estimate of the d_1^* mass, we admitted that the expected narrow γ -peak is positioned at the center of the observed structure and thus obtained $M_R \sim 1920$ MeV. However, if the uncertainty in the position of the narrow γ -peak in the structure is taken into account, the actual d_1^* mass might be considerably different from such a crude estimate. The possible existence of this dibaryon resonance was also probed in the proton-proton bremsstrahlung data taken by the WASA/Promice Collaboration at the CELSIUS accelerator[12] for proton energies of 200 and 310 MeV. However, the trigger used in those experimental studies to select events was designed and optimized for investigating the usual $pp \rightarrow pp\gamma$ bremsstrahlung. The selected events were those corresponding to two simultaneously detected protons emerging in the forward direction at angles between 4° and 20° with respect to the beam axis, each of which had a kinetic energy exceeding the present threshold (40 MeV). The analysis of those data resulted only in upper limits on the dibaryon production cross section in the mass range from 1900 to 1960 MeV. Therefore, to clarify the situation with the dibaryon resonance d_1^* , we have decided to measure the energy spectrum of the $pp \rightarrow pp\gamma\gamma$ reaction more carefully.

2 Experimental details and event selection

The experiment was performed using the variable energy proton beam from the phasotron at the Joint Institute for Nuclear Research (JINR). The schematic layout of the experimental setup is shown in Fig. 1. The pulsed proton beam

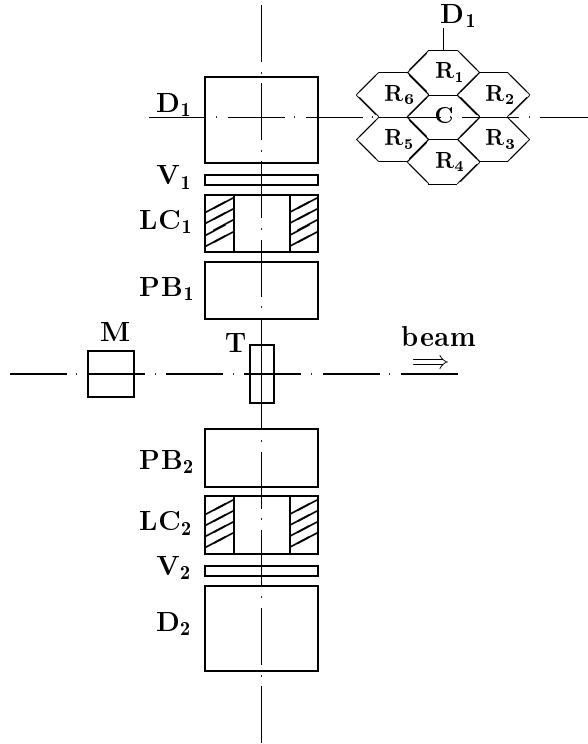


Figure 1: Experimental layout. Proton beam approaches from the left. M is the monitor of the incident beam, T is the target, D_1 and D_2 are the γ -ray detectors, V_1 and V_2 are the plastic scintillators, LC_1 and LC_2 are the lead collimators, PB_1 and PB_2 are the polyethylene bars. At the top right of the figure the cross section of the γ -ray detector D_1 is shown. C is the central detector module and R_1, R_2, \dots, R_6 (ring) are the detector modules surrounding the detector module C .

(bursts of about 7 ns FWHM separated by 70 ns) with an energy of about 216 MeV and an energy spread of about 1.5% bombarded a liquid hydrogen target (T). The average beam intensity was on the order of $3.6 \cdot 10^8$ protons/s and was monitored by an ionization chamber (M). The liquid hydrogen target was a cylindrical cryogenic vessel with a length of about 5 cm ($\sim 0.35 \text{ g/cm}^2$) and a diameter of 4.5 cm, which had thin entrance and exit windows made from 100 μm thick mylar foil. Both γ -quanta of the reaction $pp\gamma\gamma$ were detected by two γ -ray detectors (D_1 and D_2) placed in a horizontal plane, symmetrically on either side of the beam at a laboratory angle of 90° with respect to the beam direction. The γ -detector D_1 was an array of seven individual detector modules (see Fig. 1): the central detector

module (C) and six detector modules (R_1, R_2, \dots, R_6) surrounding the central detector module. Each detector module was a 15 cm thick $CsI(Tl)$ crystal having a hexagonal cross section with an outer diameter of 10 cm. The detector modules R_1, R_2, \dots, R_6 (ring) were designed to measure the energy of secondary particles and photons leaving the central detector module C . Thus, the energy of each photon detected by the detector D_1 was determined by summing up the energy deposited in the central detector module and the energies deposited in the detector modules of the ring. Besides, the ring was used as an active shielding from cosmic ray muons. The shielding was based on the fact that a cosmic ray muon that passed through the detector D_1 should deposit an energy at least greater than 50 MeV in the ring. The energy resolution of a single $CsI(Tl)$ crystal was measured to be about 13% for $E_\gamma = 15.1$ MeV. The second γ -ray detector D_2 was a cylindrical $NaI(Tl)$ crystal 15 cm in diameter and 10 cm in length. Compared to the detector D_1 , it had a poorer energy resolution for γ -rays with energies $E_\gamma > 10$ MeV. The detector D_2 was mainly designed to select $\gamma - \gamma$ coincidence events. To reject events induced by charged particles, plastic scintillators (V_1 and V_2) were put in front of each γ -detector. Both γ -ray detectors were placed in lead houses with walls 10 cm thick which were in turn surrounded by a 5 cm borated paraffin shield. The front wall of every lead house had an opening that served as a collimator (LC_1 and LC_2) limiting the angle acceptance of the γ -detector. The solid angles covered by the detectors D_1 and D_2 were 43 msr and 76 msr, respectively. To attenuate prompt particles coming from the target, 15 cm polyethylene bars (PB_1 and PB_2) were placed in between the target and each γ -detector.

The electronics associated with the γ -detectors and the plastic scintillators provided amplitude and time signals suitable for digitizing by an ADC and a TDC . The energy threshold for both the detector module C and the γ -detector D_2 was set at about 7 MeV. The amplitude signals from the γ -detectors were sent to the $ADCs$. The time signals from the γ -detectors and the plastic scintillators were sent to the $TDCs$. In addition, the radio-frequency (RF) signals from the accelerator were also sent to the TDC. Each of these signals was related with the time of arrival of the proton beam burst at the target. Therefore, the time spectrum of the RF-signals provided the means to select those events which correlate with proton bursts. The time signal from the detector module C started all the $TDCs$ and opened the ADC gates. In parallel, the time signals from the detector module C and the γ -detector D_2 were sent to a coincidence circuit to select those events which had signals from both the γ -detectors within a 250 ns time interval. The data acquisition system was triggered by signals from the coincidence circuit and the corresponding events were recorded in the event-by-event mode

on the hard disk of the computer. A further selection of $\gamma - \gamma$ coincidence candidate events was done during off-line data processing. The time interval of 250 ns was chosen to record two different types of events, "prompt" and "delayed". A prompt event is that in which both photons are due to the same beam burst. Such events may be attributed to either real $\gamma - \gamma$ events or to random coincidences. A delayed event is that in which photons are due to two different beam bursts, and, therefore, it must be attributed to a random coincidence. This type of events permits one to derive the component of random coincidences mixed with real prompt $\gamma - \gamma$ events.

Data were taken for the target filled with liquid hydrogen and for the empty one. The off-line analysis of both data sets was done in exactly the same way. The selection procedure for events associated with the process $pp \rightarrow \gamma\gamma X$ included the following main operations:

- Rejection of events induced by charge particles coming from the target. For this purpose, all events having appropriate time information from any plastic scintillators were rejected.
- Rejection of events induced by cosmic ray muons. These events were rejected by a requirement that in every event the energy detected by the ring should not exceed 30 MeV. The number of events induced by cosmic ray muons was found to be insignificant.
- Selection of events which are caused by proton beam bursts. This procedure was done with the help of a time spectrum of RF-signals. An example of this spectrum for a measurement with the full target is shown in Fig. 2. The time spectrum of RF-signals consisted of a peak of useful events superimposed on a background of events due to random coincidences. The time region confining the peak of useful events was determined, and events outside of this region were considered as a background and were rejected.
- Selection of events associated with $\gamma - \gamma$ coincidences. To do this, a spectrum of time signals from the detector D_2 (coincidence time spectrum) was used. A part of this spectrum for a measurement with the full target including the peak of prompt events and one of the peaks of delayed events is shown in Fig. 3. The coincidence time spectrum consisted of the peak of prompt events and a few peaks of delayed events. The time region confining the prompt peak was determined, and events associated with it were considered as $\gamma - \gamma$ coincidence events and were accepted.

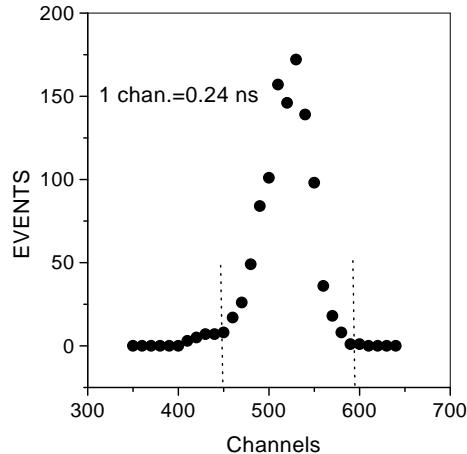


Figure 2: Time spectrum of RF-signals. The dashed lines indicate the time interval confining the peak of useful events.

3 Results and discussion

Data for the full and empty target were taken in two successive runs for ~ 31 h and ~ 21 h, respectively. The integrated luminosity of about 8.5 pb^{-1} was accumulated for the measurement with the full target. The resulting energy spectra of prompt $\gamma - \gamma$ events as a function of the photon energy measured by the detector D_1 for the full and the empty target are presented in Fig. 4. Apart from real $\gamma - \gamma$ events, these spectra also contain the contributions due to random coincidences which were determined by using delayed events. Such contributions to the full- and empty-target spectra were found to be identical within the statistical errors. The contribution of the random coincidence background to the empty-target spectrum of prompt $\gamma - \gamma$ events was less than 20%. The behavior of the empty-target spectrum is determined by photon pairs produced in collisions of protons with the mylar windows of the target vessel. Since carbon is the major component of mylar, we also performed the measurement with the carbon target to make sure that the observed shape of the empty-target spectrum is due to the process $^{12}\text{C}(p, \gamma\gamma)X$. It was found that the empty- and carbon-target spectra have the same shape.

The photon energy spectrum of the process $pp \rightarrow \gamma\gamma X$ obtained after subtraction of the empty target contribution is shown in Fig. 5. As can be seen, this spectrum consists of a narrow peak at a photon energy of about 24 MeV and a relatively broad peak in the energy range from about 50 to about 70 MeV. The statistical significance expressed in the number of

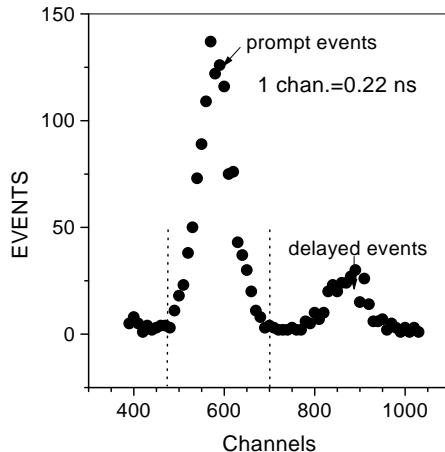


Figure 3: Coincidence time spectrum. The dashed lines indicate the time interval confining the peak of prompt events.

standard deviations (N.S.D.) was calculated for both the sharp and the broad peak using the expression $N.S.D. = (\sum_i 1/N_i^{eff}/\sigma_i^2)/(\sum_i 1/\sigma_i^2)^{1/2}$, where N_i^{eff} and σ_i are the number of events and the error bar at the energy E_i , respectively. As a result, we found that the number of standard deviations is equal to 5.3 for the narrow peak and to 3.5 for the broad peak. The width (FWHM) of the narrow peak was found to be about 8 MeV. This width is comparable with that of the energy resolution of the experimental setup. It is important to note that the number of events in the narrow peak (~ 130) is approximately equal to half the total number of events in the spectrum (~ 250). The observed behavior of the photon energy spectrum agrees with a characteristic signature of the sought dibaryon resonance d_1^* that is formed and decays in the radiative process $pp \rightarrow \gamma d_1^* \rightarrow pp\gamma\gamma$. In that case the narrow peak should be attributed to the formation of this dibaryon, while the broad peak should be assigned to its three-particle decay. Using the value for the energy of the narrow peak $E_R \sim 24$ MeV, we obtained the d_1^* mass $M_R \sim 1956$ MeV. The uncertainty of the given value is primarily due to the uncertainties in the value of the proton beam momentum and the energy of the narrow γ -peak. We estimate the total uncertainty in the d_1^* mass to be ± 6 MeV. In such a way we obtain $M_R = 1956 \pm 6$ MeV. This result is inconsistent with the rough estimate of the d_1^* mass $M_R \sim 1920$ MeV we obtained earlier[10, 11]. The results of the present experiment enable us to estimate the differential cross section of the resonance production of two

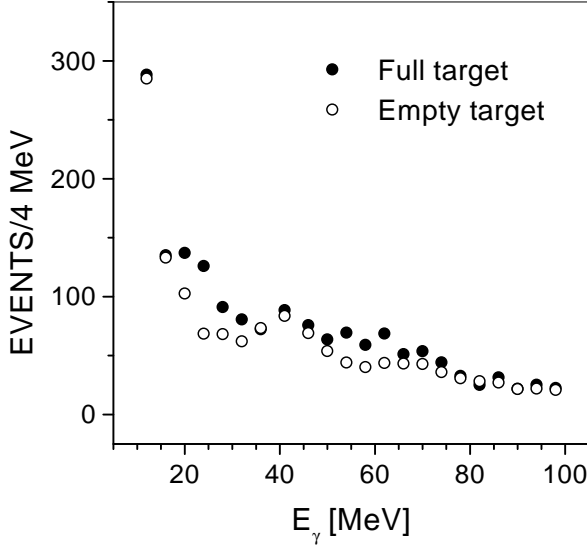


Figure 4: The photon energy spectra of prompt $\gamma - \gamma$ events for data taken with the full target (filled circles) and the empty target (open circles).

photons in the process $pp \rightarrow \gamma d_1^* \rightarrow pp\gamma\gamma$ by the formula:

$$\frac{d^2\sigma}{d\Omega_1 d\Omega_2} = \frac{N^{eff}}{L\Delta\Omega_1\Delta\Omega_2}, \quad (1)$$

where N^{eff} is the total number of events observed, L is the luminosity, and $\Delta\Omega_1$ and $\Delta\Omega_2$ are the solid angles covered by the γ -ray detectors. We found that at an energy of 216 MeV this cross section for photons emitted symmetrically at $\theta_{lab} = \pm 90^\circ$ is ~ 9 nb/sr².

Having assumed that the $pp \rightarrow \gamma d_1^* \rightarrow pp\gamma\gamma$ process with the d_1^* mass of 1956 MeV is the only mechanism of the reaction $pp \rightarrow pp\gamma\gamma$, we calculated the photon energy spectra of this reaction for a proton energy of 216 MeV. It was also assumed that the radiative decay of the d_1^* is a dipole $E1(M1)$ transition from the two-baryon resonance state to a pp -state in the continuum. The calculations were carried out with the help of Monte Carlo simulations which included the geometry and the energy resolution of the actual experimental setup. The photon energy spectra were calculated for two different scenarios of the d_1^* decay. The difference between them was that one of these scenarios took into account the final state interaction (FSI) of two outgoing protons whereas in the other that interaction was switched off. Each of the scenarios imposed some restrictions on possible quantum numbers of the dibaryon state in question. The scenario including the FSI implies that the final pp -system is in the singlet 1S_0 state and consequently it should take place, in

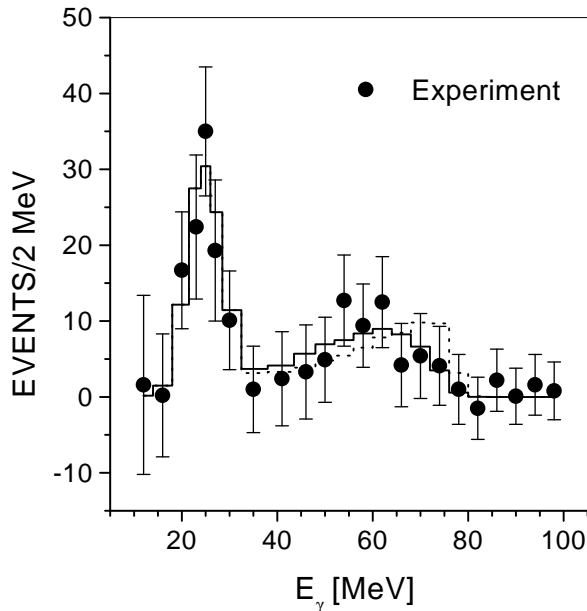


Figure 5: Experimentally observed energy spectrum for photons from the $pp\gamma\gamma$ process and energy spectra for photons from the process $pp \rightarrow \gamma d_1^* \rightarrow \gamma\gamma pp$ calculated with the help of Monte Carlo simulations for two d_1^* decay scenarios: without the FSI (solid line) and with the FSI (dashed line). The solid and dashed lines are overlapped in the energy ranges $E_\gamma \leq 30$ MeV and $E_\gamma \geq 80$ MeV.

particular, for the isovector 1^+ dibaryon state (the simplest exotic quantum numbers), namely, $1^+ \xrightarrow{M1} 0^+$. Moreover such a scenario can take place for any isotensor dibaryon state with the exception of the 0^+ or 0^- state. At the same time, the scenario in which the *FSI* is switched off, is most likely to occur for the isotensor 0^\pm dibaryon state. The spectra calculated for these two decay scenarios and normalized to the total number of $\gamma - \gamma$ events observed in the present experiment are shown in Fig.5. Comparison of these spectra with the experimental spectrum indicates that both the calculated spectra are in reasonable agreement with the experimental one within experimental uncertainties. In other words, the statistics of the experiment is insufficient to draw any firm conclusions in favor of one of these scenarios and thereby to limit possible quantum numbers of the observed dibaryon state. In this connection, we would like to emphasize that the experimental data on the process $\pi^- d \rightarrow \gamma\gamma X$ can shed some light on the properties of the dibaryon state we have observed. The point is that the d_1^* dibaryon can in principle be excited in this process via the mode $\pi^- d \rightarrow \gamma d_1^* \rightarrow \gamma\gamma nn$.

However, excitation of the dibaryon d_1^* with isospin $I = 1$ is allowed by the isospin selection rules, whereas excitation of the isotensor ($I = 2$) resonance is expected to be strongly suppressed[14, 15]. Therefore, the preliminary results of the study of the reaction $\pi^-d \rightarrow \gamma\gamma X$ carried out by the RMC Collaboration at TRIUMF[13] indicating no enhancement of the two-photon yield in the process $(\pi^-d)_{atom} \rightarrow \gamma\gamma nn$ compared to the usual one-nucleon mechanism $\pi^-p \rightarrow \gamma\gamma n$ on the proton bound in the deuteron may imply that the d_1^* dibaryon has isospin 2.

Finally, as we have already mentioned in the Introduction, the presence of the $pp \rightarrow \gamma d_1^*(1920) \rightarrow \gamma\gamma pp$ process was sought in the Uppsala pp -bremsstrahlung data[12]. Based on the detailed data analysis the authors[12] conclude that they have found no evidence for a dibaryon in the mass range from 1900 to 1960 MeV. There is, however, one important feature of the process in question which was omitted in Ref.[12]. It is related to the angular distribution of protons from the dibaryon decay $d_1^* \rightarrow pp\gamma$. The authors[12] assumed that such a distribution is isotropic in the center-of-mass system of the reaction. However, that is not the case. To understand the angular distribution of the protons from the process $pp \rightarrow \gamma d_1^*(1956) \rightarrow \gamma\gamma pp$ we performed phase space calculations using the CERN code[16]. The calculations were done for two possible decay modes of the dibaryon. One is the dibaryon decay to the singlet 1S_0 two-proton state ($^1S_0\{pp\}$). It is allowed, for instance, for d_1^* with quantum numbers $1(1^+)$ or $2(1^\pm)$. The second implies that the dibaryon decays to any other two-proton state. It was also assumed that the γ -radiation from the given process has a dipole character. The results of the calculations (in the laboratory) for an incident energy of 310 MeV and for the case when the polar angle of observed photons was constrained to the range between 30° and 90° (γ -ray detector arrangement in the Uppsala experiment) are shown in Fig.6. The same calculations done at 200 MeV led to similar results. As can be seen from Fig.6, the protons from the process $pp \rightarrow \gamma d_1^*(1956) \rightarrow \gamma\gamma ^1S_0\{pp\}$ are mainly concentrated in a narrow angular cone at $\theta_{lab} \leq 4^\circ$. Since in the Uppsala experiment events were only accepted if the polar angle of each proton fell within a forward cone between 4° and 20° , the dominant portion of events associated with the given process was beyond this angular range and, hence, were not present in the analyzed data[12]. In other words, if we assume that the $d_1^*(1956)$ has quantum numbers such as $1(1^+)$ or $2(1^\pm)$, then these data can contain only such events from the process $pp \rightarrow \gamma d_1^*(1956) \rightarrow \gamma\gamma g^1S_0\{pp\}$ in which both final protons are associated with the tail of the angular distribution presented in Fig.6. Our naive estimations have shown that the fraction of these events in the data[12] for 200 MeV and 310 MeV with respect to the corresponding total number of events from the process of interest are approximately

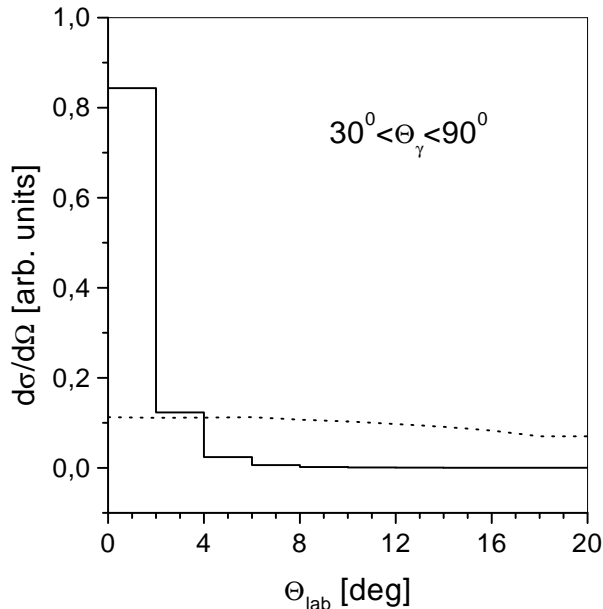


Figure 6: The angular distribution of the protons (in the laboratory) from the process $pp \rightarrow \gamma d_1^*(1956) \rightarrow \gamma\gamma pp$ calculated with FOWL[16] for the case when the polar angle of observed photons is constrained to the range between 30° and 90° . The solid line corresponds to four-body phase space with 1S_0 FSI and the dashed line to that without the FSI between the outgoing protons.

smaller than 20% and 2%, respectively. These estimates together with the differential cross section ($\frac{d^2\sigma}{d\Omega_1 d\Omega_2}$) obtained in the present experiment permitted us, in turn, to estimate the expected number of events in the Uppsala experiment. The corresponding values for the measurements at 200 MeV and 310 MeV are equal to ~ 2 and ~ 130 , respectively. It was assumed in those calculations that the energy dependence of the cross section is E_R^3 (dipole radiation), where $E_R = (s - M_R^2)/2\sqrt{s}$. Our estimate for 200 MeV is in agreement with the corresponding null result obtained in the Uppsala measurements. As for the result at 310 MeV, we would like to note the following. First, the experimental sensitivity of the data[12] at 310 MeV to the process in question was limited by a large background stemming from π^0 decays. We found that cuts applied in Ref.[12] to remove this background reduced the number of dibaryon candidates observed by a factor of ~ 3 . Second, the presence of a narrow dibaryon should appear in the $pp\gamma$ invariant mass spectrum as a sharp peak and a wider one (mirror) that arises because of the $pp\gamma$ invariant mass calculation with a photon originating from a dibaryon

production. The authors[12] believed that inside a range of dibaryon masses from 1900 to 1960 MeV these peaks would be well separated from one another. Therefore, as a signal for dibaryon production they hoped to observe a sharp peak ~ 5 MeV wide. To find the invariant mass distribution of $pp\gamma$ events from the $pp \rightarrow \gamma d_1^*(1956) \rightarrow \gamma\gamma pp$ process at 310 MeV we performed a Monte Carlo simulation of the WASA/PROMICE experimental setup. It appeared that a broad mirror and a sharp peak merge in this distribution and it consists of one wide peak extending from ~ 1943 to ~ 1968 MeV. We think that in Ref.[12] such a peak could be overlooked. Of course, the estimates obtained for the expected number of events in the Uppsala experiment are very approximate. To make more precise estimates it is desirable to have a consistent description of the $pp \rightarrow \gamma d_1^* \rightarrow \gamma\gamma pp$ process.

4 Conclusion

The γ -ray energy spectrum for the $pp \rightarrow \gamma\gamma X$ reaction at a proton energy below the pion production threshold has been measured for the first time. The spectrum measured at an energy of about 216 MeV for coincident photons emitted at an angle of 90° in the laboratory frame clearly evidences the existence of the NN -decoupled dibaryon resonance d_1^* with a mass of 1956 ± 6 MeV that is formed and decays in the process $pp \rightarrow \gamma d_1^* \rightarrow pp\gamma\gamma$. The data we have obtained, however, are still incomplete, and additional careful studies of the reaction $pp \rightarrow pp\gamma\gamma$ are needed to get proper parameters (mass, width, spin, etc.) of the observed dibaryon state.

References

- [1] S.B. Gerasimov and A.S. Khrykin, *Mod.Phys.Lett.* **A8**,2457(1993).
- [2] S.B. Gerasimov, S.N. Ershov, A.S. Khrykin, *Phys.At.Nucl.* **58**,844(1995).
- [3] P.J. Mülders, A.T. Aerts, and J.J. de Swart, *Phys.Rev.* **D 21**, 2653(1980).
- [4] L.A. Kondratyuk, B.V. Martem'yanov, and M.G. Shchepkin, *Sov.J.Nucl.Phys.* **45**, 776(1987).
- [5] V.B. Kopeliovich, *Phys.At.Nucl.* **56**,1084(1993); **58**,1237(1995).
- [6] B. Tatischeff, J. Yonnet, M. Boivin, M.P. Comets, P. Courtat, R. Gacougnolle, Y. Le Bornec, E. Loireleux, F. Reide, and N. Wills, *Phys.Rev.* **C59**,1878(1999).

- [7] W. Brodowski et al., *Z.Phys.* **A355**,5(1996).
- [8] R. Bilger, *Nucl.Phys.* **A629**,141c(1998).
- [9] L.V. Fil'kov, V.I. Kashevarov, E.S. Konobeevski, M.V. Mordovskoy, S.I. Potashev, and V.M. Shorkin, *Phys.Rev.C* **61**,044004(2000).
- [10] A.S.Khrykin, in *Proceeding of the XIV International conference on particles and nuclei (PANIC96)*, Williamisburg, Virginia,USA,1996, ed. by Carl E.Carlson and John J.Domingo,p.533.
- [11] A.S.Khrykin, in *Proceeding of the Seventh International Symposium on Meson-Nucleon Physics and the Structure of the Nucleon*, Vancouver, B.C., Canada, 1997, ed. by D.Drechsel, G.Höhler, W.Kluge and B.M.K.Nefkens, p.250.
- [12] H.Calén et al., *Phys.Lett.* **B427**,248(1998).
- [13] P.A. Zolnierczuk (The RMC Collaboration), *Acta Phys.Polon.* **B31**, 2349(2000); nucl-ex/0007011.
- [14] S.B.Gerasimov, in: *Proc. of the 13-th Int. Seminar on High Energy Physics Problems "Relativistic Nuclear Physics and Quantum Chromodynamics"*, edited by A.M. Baldin and V.V. Burov,Dubna,1998,v.II,p.3; nucl-th/9712064 and nucl-th/9812077.
- [15] S.B.Gerasimov,in *Hadronic Atoms and Positronium in the Standard Model (Proc. of the Int.Workshop)*, Dubna,26-31 May, 1998,edited M.A. Ivanov et al.,p.91; nucl-th/9808070.
- [16] F.James,"FOWL – A General Monte -Carlo Phase Space Program,"CERN Library,(1977).